



Copper adhesive-tapes for the assembly of electrodes and miniaturized cells for the detection of nitrates, nitrites and glucose

Michele Abate, Francesca Picco, Gino Bontempelli, Nicolò Dossi*

Sustainable Analytical Instrumentation Laboratory (Sustain Lab), Department of Agrifood, Environmental and Animal Science, University of Udine, via Cotonificio 108, I-33100 Udine, Italy

ARTICLE INFO

Keywords:

Copper adhesive-tape electrodes
Pencil drawn electrodes
Miniaturized electroanalytical cells
Non-enzymatic glucose sensors
Nitrate and nitrite detection

ABSTRACT

A simple and replicable approach based on the use of a cutting plotter is here presented for assembling copper electrodes by adopting adhesive copper tapes. The behavior of these Cu adhesive-tape electrodes thus assembled was first compared with that of commercial Cu-disk electrodes in conventional cells. This comparison led to completely coincident results, even if in both cases it was necessary to subject the surface of copper electrodes to an electrochemical pre-treatment. Subsequently, a quite similar approach was used to build miniaturized electrochemical cells suitable for the analysis of microvolumes of samples where reference and counter electrodes were pencil drawn. In order to evaluate thoroughly the performance of these Cu adhesive-tape electrodes, they were adopted for the nonenzymatic determination of glucose in basic medium and for the detection of nitrates and nitrites in acid medium by achieving totally satisfactory findings. The miniaturized electrochemical cell was instead successfully used only for the detection of glucose in a basic medium, since the detection of nitrates and nitrites in an acid medium required preliminary deaeration to remove atmospheric oxygen, which is an impossible operation in the miniaturized electrochemical cell. This glucose detection was also performed in a real sample consisting of a rehydration solution purchased from a local pharmacy. This paper reports the satisfactory results found in this investigation.

1. Introduction

In recent decades the need to meet sustainability requirements has also posed crucial challenges in the field of analytical chemistry, promoting the development of portable analytical devices that combine reliability and robustness with low costs and reduced use of chemicals [1–3]. In this context, miniaturized electroanalytical devices with embedded electrodes arranged in a planar configuration effectively meet these needs as they allow operation with microvolumes of sample, reducing waste production and ensuring greater operator safety [4,5].

Among the most commonly used materials for the production of these devices are carbon-based materials, including graphite, carbon black, nanotubes, and graphene. These are incorporated into ink or paste formulations used to deposit conductive traces on ceramic or plastic substrates, as well as paper and cotton, using screen printing or direct writing approaches such as inkjet or aerosol printing [6–8]. Carbon-based materials can also be mixed with clay to form hard rods commercially known as pencil leads which can be used to create conductive traces by simple abrasion on various surfaces [9–11]. Clay

can be replaced with polymer frameworks as in thin leads for micro-pencil [12,13] or conductive filaments for 3D printing, where PLA, TPU, and ABS can be mixed with carbon-based materials, thus enabling the assembling of electrochemical cells using the Fused Deposition Modeling (FDM) technology [14–16]. Although electrodes made with these materials are characterized by low cost, good conductivity and can operate over a wide potential range, there remains the need to use metals such as platinum, gold, palladium, silver, and iridium as electrodes, as these metals are widely used since key materials due to their catalytic properties, often attributable to the ultrathin metal oxide films that form spontaneously or are generated electrochemically at the electrode-solution interface [17–19].

Among these metals, copper is an inexpensive material that is abundant in the Earth's crust and suitable for electrode construction due to its high conductivity and the ability to regenerate and modify its surface [20–22]. Thanks to the formation of oxides with different oxidation states with low solubility on the electrode surface, copper exhibits electrocatalytic activity against a wide range of inorganic and organic substances. Copper oxide nanostructures can be produced

* Corresponding author.

E-mail address: nicolo.dossi@uniud.it (N. Dossi).

directly in situ on the electrode surface or synthesized ex situ and then applied to the conductive substrate, for example by drop casting [23–26].

The electrocatalytic activity of copper is exploited, for instance, for the determination of nitrates through a reduction process that leads to the formation of various intermediate products such as nitrites, hydrazine, hydroxylamine, ammonia, nitrogen, and other oxygen-containing nitrogen species. This reduction is generally carried out in acid media because the presence of protons favors the electrocatalytic reduction of nitrate on copper surfaces [27–30].

The use of copper electrodes is also envisioned in the fourth-generation electrochemical glucose sensors (FGGS) [31]. In particular, the exploitation of copper and its oxides produced under alkaline conditions represent a promising and more cost-effective alternative to other electroanalytical devices based on noble metals such as platinum, palladium, and gold. Furthermore, compared to biosensors, they do not require the use of enzymes which suffer from significant limitations due to their immobilization on solid electrodes, causing sensor instability which is also affected by environmental conditions such as pH, temperature, and humidity [32].

In general, copper can be used to make working electrodes either as a natural material, using fibers, wires or sheets, or as a thin film electrode deposited in situ or ex situ on metal or carbon-based electrodes using a Cu(II) containing acid electrolyte [33–36].

As with other metals, copper microstructures or nanostructures can be added to conductive ink or filament formulations, or they can be generated through other approaches, such as electrodeposition or laser sintering [37–39]. Methods used to deposit pure copper thin films for use as electrodes in planar electrochemical cells often require complex and energy-intensive instrumentation, such as chemical vapor deposition (CVD) and physical vapor deposition (PVD). Clearly, in this context, there is growing interest in researching alternative approaches, such as 3D printing or printed circuit board (PCB) technology for assembling copper-based electrodes for electrochemical sensors and sensing platforms [40].

In this work, adhesive copper tapes were adopted to make electrodes for electroanalytical applications using a simple construction approach based on the use of a cutting plotter. The electrochemical behavior of the assembled electrodes was first compared with that of commercial Cu-disk electrodes. They were used in a conventional cell containing a platinum counter electrode and a Ag/AgCl, 3 M KCl reference electrode, first for the determination of nitrites and nitrates in acid solutions and then for the determination of glucose in basic solutions. After verifying the performance of these electrodes in a conventional cell, the same construction approach was used to build miniaturized electrochemical cells using commercial plastic tapes. The electrode was made of copper-adhesive tapes, and the counter and pseudo-reference electrodes were drawn with a pencil using the same plotter. These three-electrode cells were subsequently used to determine glucose in synthetic samples and in a real sample consisting of a rehydration solution, achieving performance similar to that obtained with a conventional copper electrode.

2. Materials and methods

2.1. Reagents and instrumentation

Potassium chloride (KCl, $\geq 99.0\%$), sodium hydroxide (NaOH, $\geq 98\%$), sulphuric acid ($\text{H}_2\text{SO}_4 \geq 98\%$), sodium sulfate ($\text{Na}_2\text{SO}_4, \geq 99\%$), glucose ($\text{C}_6\text{H}_{12}\text{O}_6, \geq 99.5\%$), sucrose ($\text{C}_{12}\text{H}_{22}\text{O}_{11}, \geq 99.5\%$), sodium nitrate ($\text{NaNO}_3, \geq 99.0\%$) and sodium nitrite ($\text{NaNO}_2, \geq 97.0\%$) were purchased from Sigma-Aldrich (Sigma-Aldrich, Milano, I).

Deionized water obtained with a Purelab Flex 3 system (Elga, High Wycombe, UK) was used to prepare aqueous solutions. These consisted of 0.1 M NaOH solutions and 0.1 M Na_2SO_4 solutions the pH of which was adjusted to 2 by adding H_2SO_4 and measured using a pH meter (Crison pH -2001 Hach Lange, L'Hospitalet de Llobregat, Spain). The

standard solutions of the various analytes were prepared in deionized water to obtain a final concentration of 10 mM and were diluted when necessary to the desired concentration with the used electrolyte solution.

Electrochemical measurements were conducted with a PalmSens potentiostat (PalmSens, Houten, NL) driven by the relevant software using an Ag/AgCl, 3 M KCl reference electrode (CH Instruments, Austin, TX, USA) and a copper disk (diameter 3 mm) working electrode (DEK Research, Hong Kong).

2.2. Preparation of the real sample

To evaluate the device's performance, a glucose-containing oral rehydration solution, purchased from a local pharmacy, was used as the real sample. The sample was prepared according to the instructions on the package, i.e. by dissolving the content of each sachet (5.8 g) in 200 ml of deionized water. It was then diluted 1:200 (v/v) with the electrolyte solution for analysis.

2.3. Construction of copper adhesive-tape electrodes

Copper electrodes suitable for use in conventional cells were fabricated using a cutting plotter (Silhouette Cameo, Micronet Italia, Milan, Italy), exploiting a specially created digital design. Specifically, the release liner of the single-sided copper-based conductive tape (Nano-AndMore, Wetzlar, DE) was first removed (Fig. 1a). The copper tape was then attached to a piece of thermoplastic film (Fig. 1b), which was secured with paper adhesive tape to a flexible plastic cutting mat printed with a 2.5 cm grid to facilitate material placement and alignment. After cutting the electrodes with the blade installed on the plotter (Fig. 1c), the excess copper tape was removed (Fig. 1d) and the thermoplastic film was heat-sealed to the electrodes using a hot plate to ensure a single exposed electrode surface (Fig. 1e). Finally, the electrodes were separated from each other using a cutter (Fig. 1f) and the electrode area of each electrode was delimited by applying an insulating tape, thus obtaining an effective surface area of 12.5 mm² (Fig. 1g).

The resulting electrodes were used for conventional voltammetric measurements, carried out in an electrochemical cell (5 mL) in which an Ag/AgCl, 3 M KCl reference electrode and a platinum counter electrode were also introduced. When comparison measurements were performed, these copper adhesive tape electrodes were replaced by conventional commercial copper disk electrodes (3 mm diameter).

2.4. Construction of miniaturized copper adhesive-tape cells

Copper adhesive-tapes were also used to assemble miniaturized three-electrode cells. With this purpose, a piece of 3 M Scotch® Magic™ 810 tape was first attached to the cutting mat (Fig. 2a) and then copper tape was applied (Fig. 2b). Once the electrodes were cut with the blade installed on the plotter (Fig. 2c), the excess of copper tape was removed (Fig. 2d), leaving the copper electrodes on the Scotch® tape. After replacing the blade with mechanical micropencils loaded with Super HI-Polymer micropencil leads of grade 4B ($\varnothing = 0.5$ mm) from Pentel (Swindon, UK), the reference and counter graphite electrodes were drawn directly onto the plastic tape (Fig. 2e). Once the cells were produced, the adhesive tape was rewound and stored (Fig. 2f). Before use, each cell was fixed to a PVC support (180 μm thick) from Followes (Itasca, IL, USA) and separated from the others with the aid of a utility cutter (Fig. 2f). Thin strips of insulating adhesive tapes were placed on top of the three electrodes to delimit the active working surface and to protect electrical connections from contact with liquid samples (Fig. 2g). Mini-crocodile connectors located outside the vinyl film barrier that delimits the effective electrochemical cells were used for electrical connections to all electrodes.

These miniaturized cells were used to perform measurements on very small, controlled-volume samples (90 μL) that were applied directly to

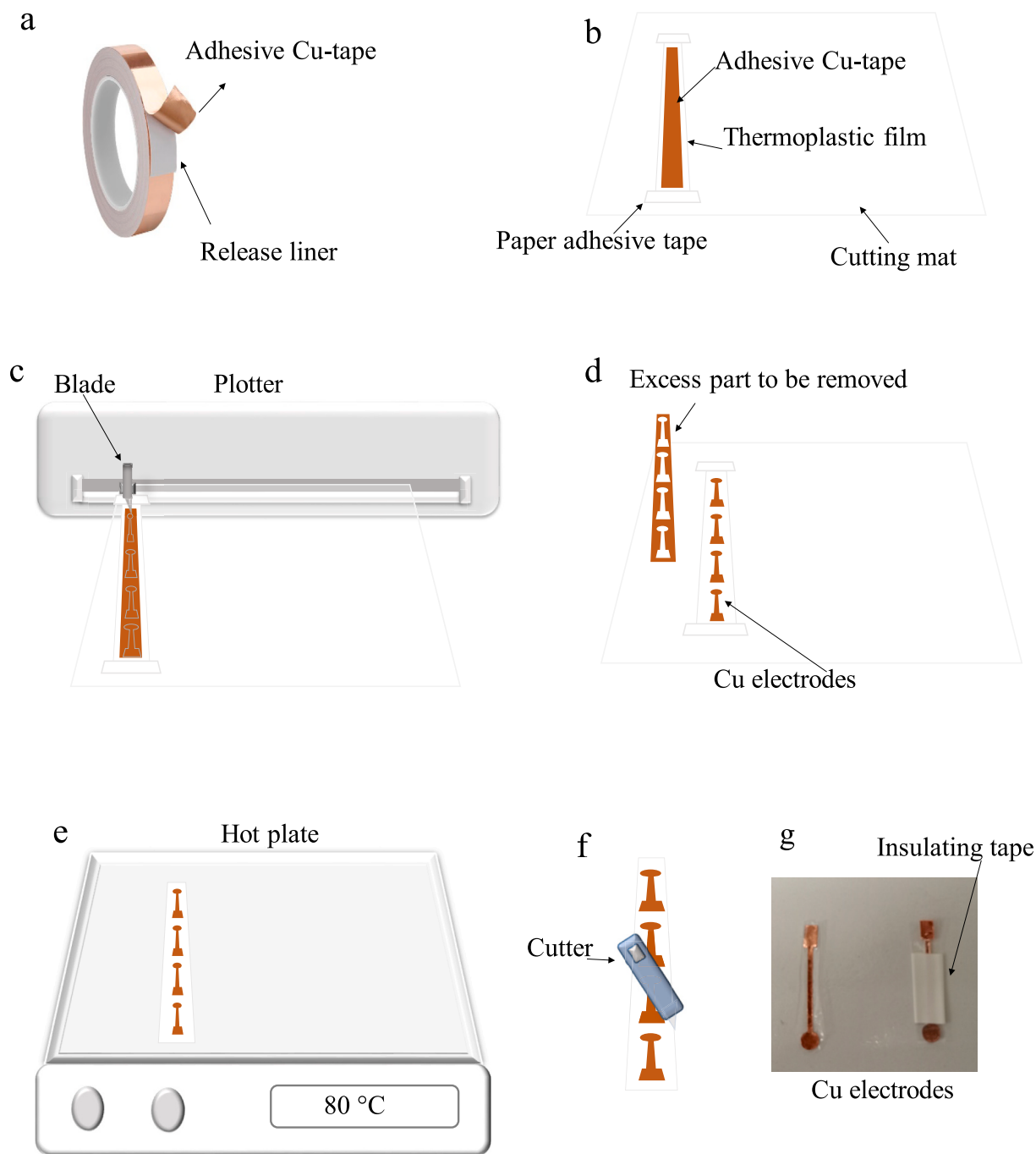


Fig. 1. Scheme of the assembly procedure of the Cu adhesive-tape electrodes (a - f) and picture of the assembled devices (g).

the cell, which was placed horizontally on a planar surface (drop mode; working electrode area approximately 12.5 mm^2).

2.5. Electrochemical measurements

Prior to conduct investigations in conventional cells involving cathodic processes, the oxygen present in the solutions was removed by degassing with a nitrogen flow for 5 min under stirring.

Before using both conventional commercial copper disk electrodes and copper-adhesive tape electrodes, it was necessary to pre-treat the copper surfaces to acquire better signals and increase the sensitivity of the measurements performed on the analytes under study. To this end, two different electrochemical procedures were adopted.

Voltammetric determinations performed in the cathodic direction

(detection of nitrates and nitrites, see Section 3.2), were performed after the electrode had been pre-treated using an electrochemical activation procedure suggested in the literature [41]. This method is based on the application to the electrode, dipped in a Na_2SO_4 solution acidified to pH 2 with H_2SO_4 , of a potential of 0.5 V vs Ag/AgCl, 3 M KCl for 10 s and subsequently of -0.25 V vs Ag/AgCl, 3 M KCl for 15 s. This procedure was repeated before each measurement.

For voltammetric determinations performed in the anodic direction (glucose detection, see Section 3.3), copper electrodes were instead pre-treated following a different procedure, also suggested in the literature [42]. This involved electrochemical activation of Cu surfaces in a 0.1 M NaOH solution, performing cyclic potential scans, repeated for 20 cycles, in a range from -1.0 V to 0.7 V vs Ag/AgCl using a scan rate of 20 mV s^{-1} .

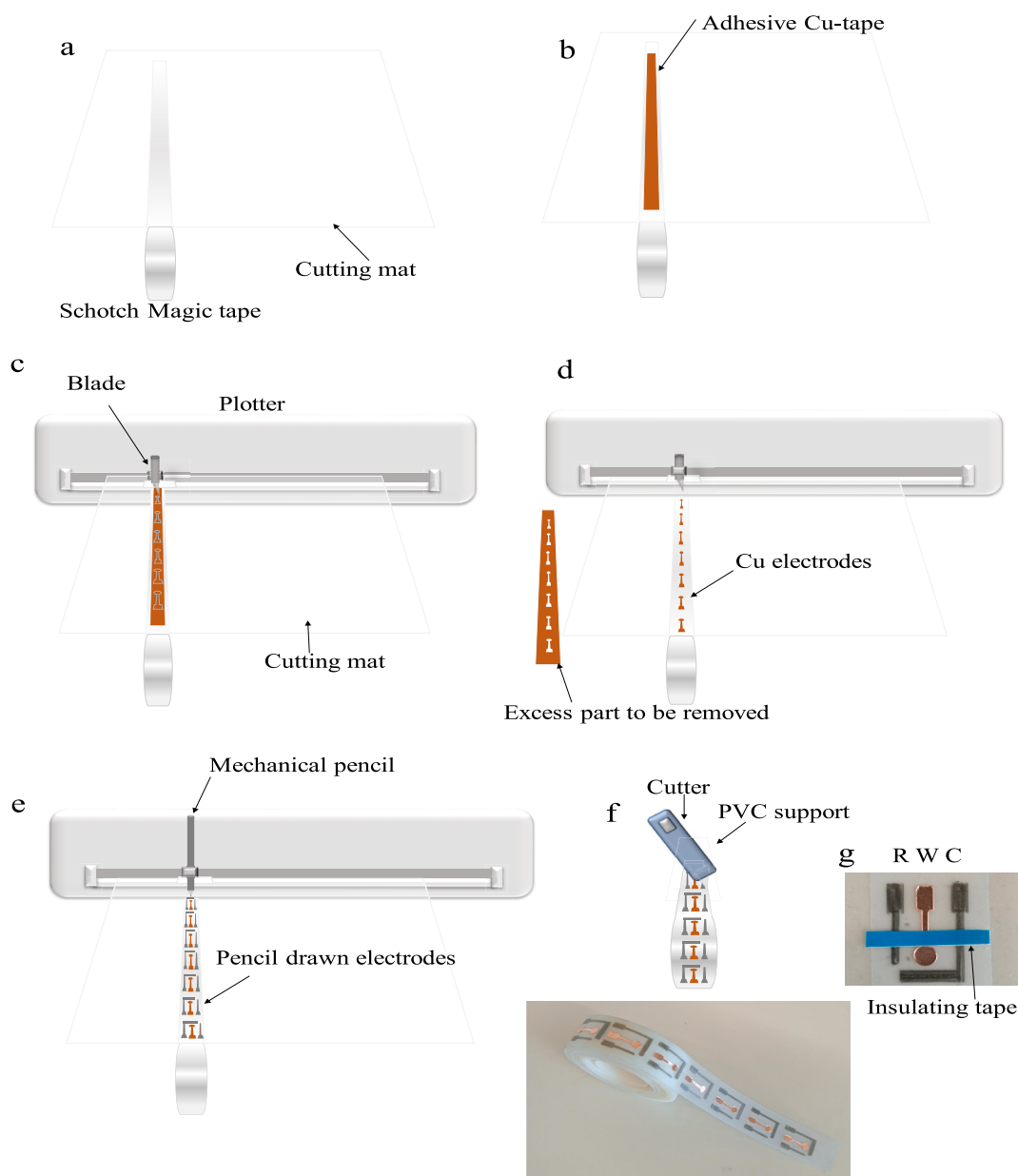


Fig. 2. Scheme of the assembly procedure of the miniaturized copper-adhesive tape cells (a - f) and picture of the assembled devices (g).

The detection of nitrates, nitrites and glucose described in the following were performed by using both Linear Sweep Voltammetry (LSV) and Square Wave Voltammetry (SWV).

The electrochemical determination of nitrates and nitrites was conducted in Na_2SO_4 solutions acidified to pH 2 with H_2SO_4 . The optimized parameters adopted for the two techniques were as follows: in the LSV technique, the potential was scanned in the range from -0.05 V to -0.7 V vs. Ag/AgCl, 3 M KCl with a scan rate of $50 \text{ mV} \cdot \text{s}^{-1}$, while in the SWV technique, a cathodic scan was applied in the potential range from -0.05 V to -0.7 V vs. Ag/AgCl, 3 M KCl, with the following parameters: potential step 5 mV, potential amplitude 30 mV, frequency 1.0 Hz.

Glucose determinations were instead carried out in a 0.1 M NaOH solution, adopting the following optimized pre-treatment parameters for the two techniques: in the LSV approach an anodic scans were performed with a scan rate of $20 \text{ mV} \cdot \text{s}^{-1}$ in the potential range from 0.0 V to 0.6 V vs. Ag/AgCl, 3 M KCl when Cu adhesive-tapes electrodes were adopted; in the SWV technique, adopted when measurements were conducted with the miniaturized Cu adhesive-tape cell, an anodic scan

was instead applied in the potential range from 0.25 V and 0.75 V vs. the graphite pseudo-reference electrode with the following parameters: potential step 5 mV, potential amplitude 30 mV and frequency 1.0 Hz.

3. Results and discussion

3.1. Comparison of Cu adhesive-tape electrodes with conventional commercial Cu disk electrodes

Cyclic voltammograms recorded in the range from -1.0 V to 0.7 V vs. Ag/AgCl, 3 M KCl using a scan rate of $20 \text{ mV} \cdot \text{s}^{-1}$ on both conventional Cu disk electrodes and Cu adhesive-tape electrodes dipped in 0.1 M NaOH aqueous solutions showed quite similar profiles with satisfactory repeatability as reported in Fig. 3.

In agreement with literature reports [42,43], the first peak recorded in the anodic direction at about -0.40 V corresponds to the oxidation process of Cu(0) to Cu(I) with the formation of a first layer of Cu(I) oxide (Cu_2O), while the second anodic peak at about -0.07 V is due to the

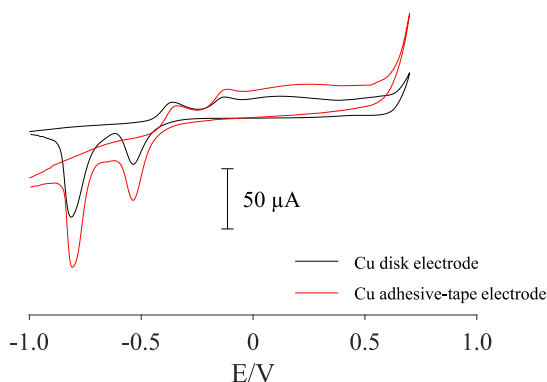


Fig. 3. Cyclic voltammograms recorded in a 0.1 M NaOH aqueous solution at a conventional Cu disk electrode (black line) and at a Cu adhesive-tape electrode (red line) in the range from -1.0 V to 0.7 V vs. Ag/AgCl, 3 M KCl using a scan rate of 20 mV s^{-1} . (For interpretation of the references to colour in this figure legend, the reader is referred to the web version of this article.)

oxidation of Cu(I) to Cu(II) with the formation of a further mixed layer of Cu(II) oxide-hydroxide (CuO/Cu(OH)₂). The subsequent wave displayed in the range from about 0 V to 0.4 V is associated to the partial dissolution of the surface films. Finally, the two cathodic peaks detectable in the reverse scan at about -0.52 V and -0.81 V are associated to the reduction of Cu(II) species to Cu(I) and of Cu(I) species to Cu(0), respectively.

It should be emphasized, however, that several investigators have highlighted the existence of different species associated with the different oxidation states of copper, making quite complex the detailed interpretation of the processes involved in the electrooxidation of copper in alkaline media. The results of their investigations suggest in fact, not only the formation of insoluble species onto the copper surface but also the occurrence of electroadsorption reactions.

Cyclic voltammograms totally coincident with those reported in Fig. 3 could also be recorded using the above mentioned miniaturized three-electrode cells, even though the potentials were shifted in the positive direction, due to the fact that they were referred to a pencil drawn graphite pseudo-reference electrode, instead of vs. Ag/AgCl, 3 M KCl reference electrode.

The comparison between Cu adhesive-tape electrodes and conventional Cu disk electrodes was also performed in acid media by evaluating their behavior in aqueous solutions of Na₂SO₄ added with H₂SO₄ to bring them to pH = 2. In order to avoid interferences caused by the presence of atmospheric oxygen, it was preliminarily removed by nitrogen flow. Voltammetric scans recorded in the cathodic region showed a behavior completely coincident between the two electrodes. Instead, the anodic region was not explored because at this pH, copper already underwent oxidation at approximately 0 V.

At this pH, no comparison was made with the miniaturized three-electrode cells mentioned above, as they did not allow a preliminary deaeration to remove atmospheric oxygen.

To further and more thoroughly evaluate the performance of the Cu adhesive-tape electrodes, we performed the two determinations reported below, one in a basic medium and the other in an acid medium.

3.2. Nitrates and nitrites detection

Reduction of nitrate and nitrite ions in acid aqueous solutions (0.1 M Na₂SO₄ + 0.01 M H₂SO₄), deaerated with nitrogen gas to remove atmospheric oxygen, did not produce well-defined and repeatable peaks at both conventional Cu disk electrodes and Cu adhesive-tape electrodes. These reductions produced instead poorly repeatable, fairly flat waves with significantly attenuated signals.

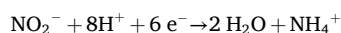
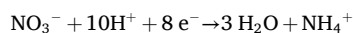
To overcome this drawback, the surface of both types of electrodes was subjected to a preliminary activation procedure already suggested

in the literature [41,44] which is based on the preliminary electrochemical dissolution of the first layer of the copper surface by applying a potential of 0.5 V for 10 s and subsequently carrying out the immediate reduction of Cu²⁺ ions, thus generated in the diffusion layer adjacent to the electrode surface, by applying a potential of -0.25 V for 15 s. After this pre-treatment, which had to be repeated before each measurement, well-defined and repeatable peaks could be recorded for both nitrites (at -0.21 V) and nitrates (at -0.47 V) on both electrodes. These peaks were better resolved when recorded by SWV, as shown in Fig. 4 which reports some voltammograms recorded for a 0.5 mM nitrate solution to which increasing concentrations of nitrites were added.

In order to evaluate the reproducibility of the assembly operations and of the electrode responses, a series of tests was carried out using different Cu adhesive-tape electrodes ($n = 5$) on the same sample consisting of a deaerated aqueous solution of 0.1 M Na₂SO₄ + 0.01 M H₂SO₄ added with 0.5 mM NO₃⁻. From these tests it was possible to deduce a RSD% equal to 4.1% .

Using square wave voltammetry (SWV), well reproducible cathodic peaks could be recorded for both nitrites and nitrates, added individually to the aqueous solution of 0.1 M Na₂SO₄ + 0.01 M H₂SO₄, whose height increased with increasing concentrations. Their height was characterized by a satisfactory linearity in the range 25 – 1500 μM for nitrates and 100 – 1000 μM for nitrites. The corresponding calibration plots turned out to be $i(\mu A) = -0.0176 C_{NO_2} + 0.4942$ ($R^2 = 0.99$) (Inset a in Fig. 4) and $i(\mu A) = -0.0598 C_{NO_3} + 0.3757$ ($R^2 = 0.99$) (Inset b in Fig. 4) for nitrites and nitrates, respectively. It was also possible to evaluate the corresponding detection limits as $3\sigma/s$ (σ is the standard deviation of the background noise and s is the sensitivity deduced from the calibration plot), which turned out to be 28.6 μM for nitrites and 7.8 μM for nitrates.

The different sensitivity observed for the two considered reduction processes is likely attributable to the different number of electrons involved. Indeed, it has been suggested that the reduction of nitrates in acid media proceeds by first transferring an O atom from nitrates to hydrogen atoms simultaneously produced in the cathodic reduction, giving rise to water and nitrite ions, which in turn are reduced to ammonium ions, according to the following reactions [41,45–47]:



3.3. Glucose detection

Linear sweep voltammograms recorded at Cu adhesive-tape electrodes not subjected to the pre-treatment activation reported in Section 2.5 and dipped in 0.1 M NaOH aqueous solutions containing 1.0 mM glucose displayed a rather low anodic peak which appeared poorly repeatable. When voltammograms were instead recorded at the same electrodes subjected to the mentioned pre-treatment process and in the absence of glucose, it was observed that the peak relative to the oxidation of Cu(I) to oxides/hydroxides of Cu(II) increased significantly with the number of pre-activation potential cycles, as shown in Fig. 5A, thus suggesting a progressive increase of the availability on the electrode surface of the species catalyzing the glucose oxidation.

When glucose was added to the solutions where the Cu electrodes were thus activated, a well-defined and repeatable anodic peak at about 0.5 V vs. Ag/AgCl, 3 M KCl was displayed, whose height increased linearly with the glucose concentration. This good repeatability observed when pre-treated electrodes were used can reasonably be attributed to a greater availability and stability of the oxide/hydroxide films formed at the copper electrode surface following the activation process.

Also in this case, the reproducibility of the assembly operations and of the electrode responses was evaluated by carrying out a series of tests using different Cu adhesive-tape electrodes ($n = 5$) dipped in the same sample consisting of a 0.1 M NaOH aqueous solution, added with 1.0

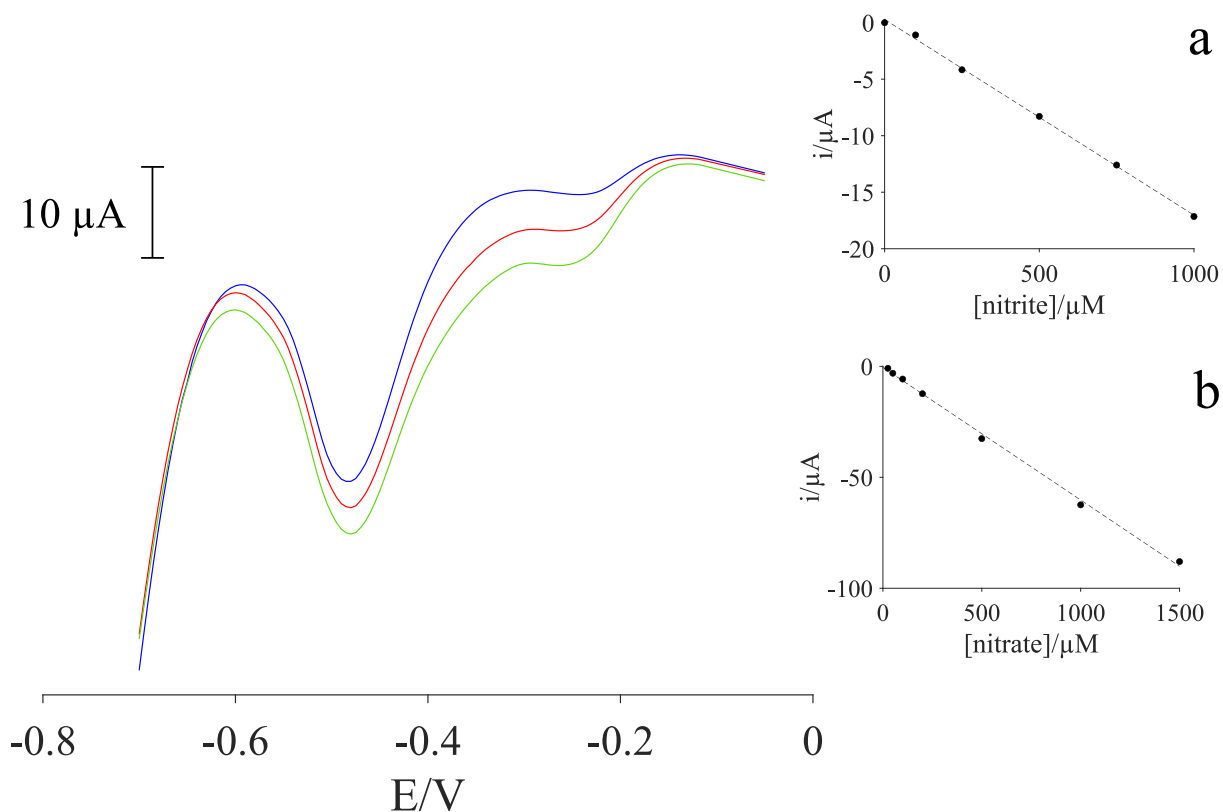


Fig. 4. Square wave voltammograms recorded at a Cu adhesive-tape electrode, subjected to the described preliminary activation procedure, in an aqueous 0.1 M $\text{Na}_2\text{SO}_4 + 0.01 \text{ M H}_2\text{SO}_4$ solution, deaerated with nitrogen gas and containing 0.50 mM NO_3^- , added with nitrite concentrations of 0.25 mM (blue line), 0.50 mM (red line) and 0.75 mM (green line). Inset a: correlation plot between current of the cathodic peak and nitrite concentration. Inset b: correlation plot between current of the cathodic peak and nitrate concentration. (For interpretation of the references to colour in this figure legend, the reader is referred to the web version of this article.)

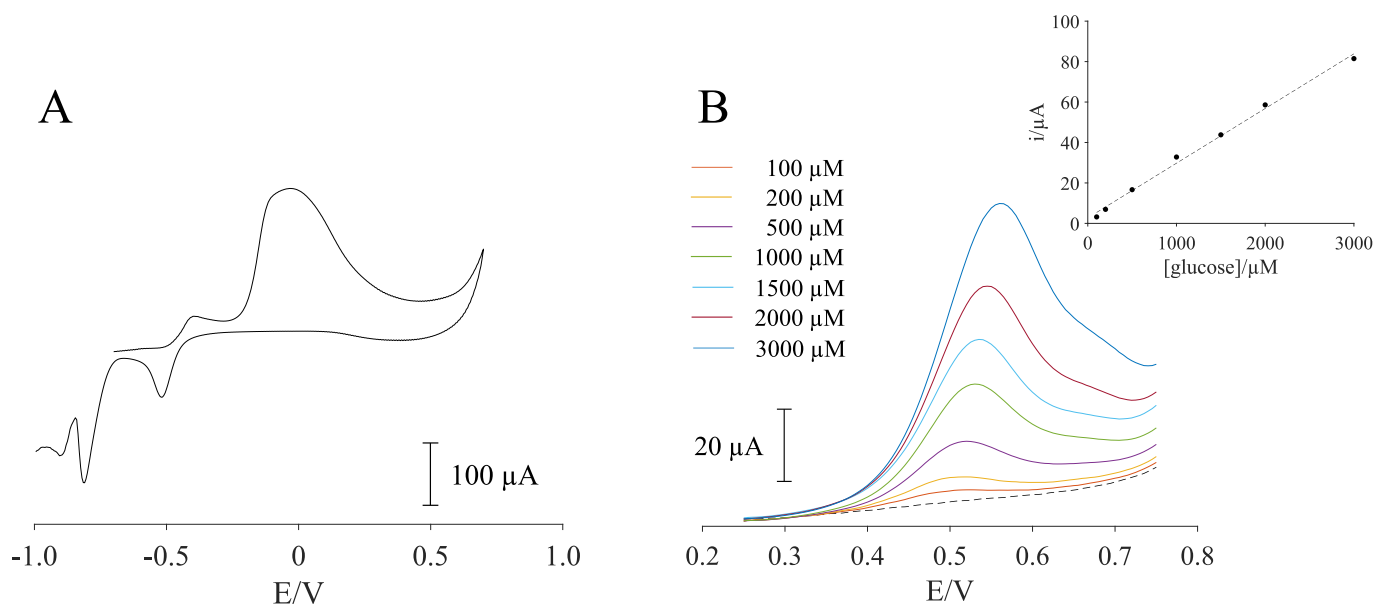


Fig. 5. A: Cyclic voltammogram recorded at a scan rate of 20 mV s^{-1} vs. an Ag/AgCl, 3 M KCl at a Cu adhesive-tape electrode dipped in 0.1 M NaOH aqueous solution, subjected to the described preliminary activation procedure consisting in cyclic potential scans repeated for 20 cycles, in an aqueous 0.1 M NaOH solution in the absence of glucose. B: SWV responses recorded in the miniaturized copper adhesive-tape cell where 90 μL of a 0.1 M NaOH solution containing the reported increasing glucose concentrations were applied. The inset reports the corresponding calibration plot. The background is reported by the dashed line.

mM glucose. From these tests it was possible to deduce a RSD% equal to 4.6%.

Subsequently, quantitative glucose determinations were performed

using the aforementioned miniaturized copper adhesive-tape cell, applying small volumes (90 μL) of the aqueous solutions under investigation to its surface, by taking advantage of the fact that these did not

require the removal of atmospheric oxygen, since they were conducted exploiting an anodic process.

The dependence of the height of the glucose oxidation peak, which turned out to increase with its concentration, was evaluated using the SWV, in order to take advantage of its greater sensitivity, also due to the fact that this technique enables the contribution of capacitive currents to be minimized.

The SWV peaks recorded in the glucose concentration range from 0.1 to 3 mM are shown in Fig. 5B, where also the corresponding calibration plot is reported as the inset. It was found to be $i(\mu\text{A}) = 0.027 C_{\text{Gluc}} + 2.608$ ($R^2 = 0.995$) (Inset in Fig. 5B). These measurements also made it possible to evaluate the corresponding detection limit as $3\sigma/s$ (σ is the standard deviation of the background noise and s is the sensitivity deduced from the calibration plot), which turned out to be 28 μM .

The calibration plot thus identified was used to verify the glucose concentration present in a real sample consisting of a glucose-containing oral rehydration solution. Preliminary voltammograms recorded on this real sample allowed us to verify that only the glucose oxidation peak appeared in the scanned potential range. This was however expected on the basis of the information provided by the ingredient list included with the real sample. To better control for the absence of any interference, controlled amounts of sucrose were added to the real sample, thus verifying that even the presence of this sugar had no effect on the glucose response.

This result is in total agreement with the expectation that the electrocatalytic activity of the copper electrode surface is only displayed on reducing sugars.

Confirming the satisfactory performance of the Cu-adhesive tape cell, repeated analysis of different aliquots of the real sample led to the conclusion that the glucose content was 624 g/kg, in satisfactory agreement ($\pm 8.7\%$) with the data reported on the manufacturer's label.

4. Conclusions

The electrodes proposed here are assembled using easily accessible materials and construction technologies that enable the construction of analytical devices that allow analyses to be performed in compliance with the fundamental principles of Green Analytical Chemistry (GAC) and Democratic Analytical Chemistry (DAC).

The design approach proposed here enables the assembly of electrodes that can be used as a valid alternative to the copper disk electrodes commonly used in electroanalytical applications. Furthermore, their geometry makes them particularly suitable for the construction of three-electrode devices similar to screen-printed electrodes (SPEs) or thin-film electrodes (TFEs). In this regard, further investigations are currently underway to integrate these electrodes into miniaturized cells with a planar configuration capable of operating with microsample volumes.

It is also worth noting that the manufacturing method adopted allows both the shape and size of the electrodes to be changed easily and quickly by simply modifying the digital design and the very quick production of large quantities (20 electrodes in approximately 30 min).

CRediT authorship contribution statement

Michele Abate: Methodology, Investigation, Formal analysis, Data curation, Conceptualization. **Francesca Picco:** Investigation, Data curation. **Gino Bontempelli:** Writing – review & editing, Writing – original draft. **Nicolò Dossi:** Writing – review & editing, Writing – original draft, Resources, Funding acquisition, Conceptualization.

Declaration of competing interest

The authors declare that they have no known competing financial interests or personal relationships that could have appeared to influence the work reported in this paper.

Data availability

Data will be made available on request.

References

- [1] C.M. Hussain, G. Hussain, R. Keçili, Disposable analytical chemistry: design, application and sustainability, *TrAC-Trends Anal. Chem.* 192 (2025) 118414, <https://doi.org/10.1016/j.trac.2025.118414>.
- [2] C. Grazioli, E. Lanza, M. Abate, G. Bontempelli, N. Dossi, Lab-on kit: a 3D printed portable device for optical and electrochemical dual-mode detection, *Talanta* 275 (2024) 26185, <https://doi.org/10.1016/j.talanta.2024.126185>.
- [3] F. Chemat, S. Garrigues, M. de la Guardia, Portability in analytical chemistry: a green and democratic way for sustainability, *Curr. Opin. Green Sustain. Chem.* 19 (2019) 94–98, <https://doi.org/10.1016/j.cogsc.2019.07.007>.
- [4] A. Sajeevan, R.A. Sukumaran, L.R. Panicker, Y.G. Kotagiri, Trends in ready-to-use portable electrochemical sensing devices for healthcare diagnosis, *Microchim. Acta* 192 (2025) 80, <https://doi.org/10.1007/s00604-024-06916-x>.
- [5] G. Paimard, E. Ghasali, M. Baeza, Screen-printed electrodes: fabrication, modification, and biosensing applications, *Chemosensors* 11 (2023) 113, <https://doi.org/10.3390/chemosensors11020113>.
- [6] L.F. Castro, F. d'Orlyé, J. Vinh, Y. Verdier, A. Varenne, Disposable carbon screen-printed electrodes for on-chip protein digestion: a proteomic approach coupled to MALDI-TOF MS, *Anal. Chem.* (2025), <https://doi.org/10.1021/acs.analchem.5c03760> in press.
- [7] J. Rocha Camargo, L.O. Orzari, D.A. Gouveia Araújo, P.R. de Oliveira, C. Kalinke, D.P. Rocha, A.L. dos Santos, R.M. Takeuch, R.A.A. Munoz, J.A. Bonacin, B. Campos Janegitz, Development of conductive inks for electrochemical sensors and biosensors, *Microchem. J.* 164 (2021) 105998, <https://doi.org/10.1016/j.microc.2021.105998>.
- [8] E. Costa-Rama, M.T. Fernández-Abedul, Paper-based screen-printed electrodes: a new generation of low-cost electroanalytical platforms, *Biosensors* 11 (2021) 51, <https://doi.org/10.3390/bios11020051>.
- [9] N. Dossi, R. Toniolo, F. Impellizzeri, G. Bontempelli, Doped pencil leads for drawing modified electrodes on paper-based electrochemical devices, *J. Electroanal. Chem.* 722–723 (2014) 90–94, <https://doi.org/10.1016/j.jelechem.2014.03.038>.
- [10] N. Dossi, R. Toniolo, A. Pizzariello, F. Impellizzeri, E. Piccin, G. Bontempelli, Pencil-drawn paper supported electrodes as simple electrochemical detectors for paper-based fluidic devices, *Electrophoresis* 34 (2013) 2085–2091, <https://doi.org/10.1002/elps.201200425>.
- [11] B. Ferreira, I.V.S. Arantes, D.P.M. Saraiva, L.A. Pradela-Filho, M. Bertotti, T.R.L. C. Paixao, Commercial ink-coated PVC: no longer abrading conventional PVC surfaces for electrode fabrication using pencil drawing, *Microchem. J.* 198 (2024) 110149, <https://doi.org/10.1016/j.microc.2024.110149>.
- [12] L. Trnkova, I. Triskova, J. Cechal, Z. Farka, Polymer pencil leads as a porous nanocomposite graphite material for electrochemical applications: the impact of chemical and thermal treatments, *Electrochem. Commun.* 126 (2021) 107018, <https://doi.org/10.1016/j.elecom.2021.107018>.
- [13] N. Dossi, R. Toniolo, F. Tubaro, R. Svelgel, G. Bontempelli, S. Petrazzi, F. Terzi, E. Piccin, Digitally controlled procedure for assembling fully drawn paper-based electroanalytical platforms, *Anal. Chem.* 89 (2017) 10454–10460, <https://doi.org/10.1021/acs.analchem.7b02521>.
- [14] L.R.G. Silva, L. Ventosa Bertolim, J.S. Stefano, J.A. Bonacin, E.M. Richter, R.A. A. Munoz, B. Campos Janegitz, New route for the production of lab-made composite filaments based on soybean oil, polylactic acid and carbon black nanoparticles, and its application in the additive manufacturing of electrochemical sensors, *Electrochim. Acta* 513 (2025) 145566, <https://doi.org/10.1016/j.electacta.2024.145566>.
- [15] C. Grazioli, R. Svelgel, N. Dossi, A novel strategy for fabrication, activation and cleaning of fully 3D printed flexible planar electrochemical platforms, *Electroanalysis* 35 (2023) e202300013, <https://doi.org/10.1002/elan.202300013>.
- [16] E. Sigley, C. Kalinke, R.D. Crapnell, M.J. Whittingham, R.J. Williams, E.M. Keefe, B. Campos Janegitz, J.A. Bonacin, C.E. Banks, Circular economy electrochemistry: creating additive manufacturing feedstocks for caffeine detection from post-industrial coffee pod waste, *ACS Sustain. Chem. Eng.* 11 (2023) 2978–2988, <https://doi.org/10.1021/acssuschemeng.2c06514>.
- [17] F. Terzi, L. Pigani, C. Zanardi, Unusual metals as electrode materials for electrochemical sensors, *Curr. Opin. Electrochem.* 16 (2019) 157–163, <https://doi.org/10.1016/j.coelec.2019.05.005>.
- [18] P.J. Obeid, N. Sari-Chmayssem, P. Yammine, D. Homs, H. El-Nakat, Z. Matar, S. Hamieh, D. Koumeir, A. Chmayssem, Designs and materials of electrodes for electrochemical sensors, *ChemElectroChem* 12 (2025) e202500230, <https://doi.org/10.1002/celec.202500230>.
- [19] Y. Lv, N. Yang, M. You, J. Hao, J. Li, M. Zhang, Treatment rather than pretreatment: electrochemical activation of electrodes for electroanalysis, *Microchem. J.* 215 (2025) 114422, <https://doi.org/10.1016/j.microc.2025.114422>.
- [20] L.Y. Martynov, O.A. Naumova, N.K. Zaitsev, I.Y. Lovchinovskiy, The use of copper indicator electrodes in voltammetric analysis, *Fine Chem. Technol.* 11 (2016) 26–41, <https://doi.org/10.32362/2410-6593-2016-11-5-26-41>.
- [21] D. Obrez, M. Kolar, N. Tasić, S.B. Hočevar, Study of different types of copper electrodes for anodic stripping voltammetric detection of trace metal ions,

- Electrochim. Acta 457 (2023) 142480, <https://doi.org/10.1016/j.electacta.2023.142480>.
- [22] M. Perez-Estebanez, L. Romay, M. Huidobro, P. Nuñez-Marinero, A. Heras, F. Javier del Campo, A. Colina, Disposable copper electrodes based on printed circuit board technology for the operando generation of Raman-enhancing substrates, *Anal. Chem.* 97 (2025) 20753–20760, <https://doi.org/10.1021/acs.analchem.5c02381>.
- [23] E. Fernández-García, P. Merino, N. González-Rodríguez, L. Martínez, M. del Pozo, J. Prieto, E. Blanco, G. Santoro, C. Quintana, M.D. Petit-Domínguez, E. Casero, L. Vázquez, J.I. Martínez, J.A. Martín-Gago, Enhanced electrocatalysis on copper nanostructures: role of the oxidation state in sulfite oxidation, *Anal. Chem.* 97 (2025) 20753–20760, <https://doi.org/10.1021/acs.analchem.5c02381>.
- [24] G. Zampardi, J. Thöming, H. Naatz, H.M.A. Amin, S. Pokhrel, L. Mädler, R. G. Compton, Electrochemical behavior of single CuO nanoparticles: implications for the assessment of their environmental fate, *Small* 14 (2018) 1801765, <https://doi.org/10.1002/sml.201801765>.
- [25] S. Qiu, C. Wu, S. Akter, S. Hong, H. Liu, S. Mahmud, Copper oxide-modified screen-printed carbon electrodes for the detection of mycobacterium tuberculosis infection treating drug: isoniazid, *Ionics* 30 (2024) 8631–8645, <https://doi.org/10.1007/s11581-024-05863-0>.
- [26] C.M. Welch, M.E. Hyde, C.E. Banks, R.G. Compton, The detection of nitrate using in-situ copper nanoparticle deposition at a boron doped diamond electrode, *Anal. Sci.* 21 (2025) 1421, <https://doi.org/10.2116/analsci.21.1421>.
- [27] J. Davis, M.J. Moorcroft, S.J. Wilkins, R.G. Compton, M.F. Cardoso, Electrochemical detection of nitrate and nitrite at a copper modified electrode, *Analyst* 125 (2000) 737–742, <https://doi.org/10.1039/A909762G>.
- [28] J. Davis, M.J. Moorcroft, S.J. Wilkins, R.G. Compton, M.F. Cardoso, Electrochemical detection of nitrate at a copper modified electrode under the influence of ultrasound, *Electroanalysis* 12 (2000) 1363–1367, [https://doi.org/10.1002/1521-4109\(200011\)12:17<1363::AID-ELAN1363>3.0.CO;2-4](https://doi.org/10.1002/1521-4109(200011)12:17<1363::AID-ELAN1363>3.0.CO;2-4).
- [29] J. Gajdar, S.R. Gaspar, M.G. Almeida, Trends in nitrite detection: recent advances in electrochemical sensor technologies, *TrAC-Trends Anal. Chem.* 183 (2025) 118105, <https://doi.org/10.1016/j.trac.2024.118105>.
- [30] X. Luo, J. Wu, Y. Ying, Voltammetric detection of nitrate in water sample based on in situ copper-modified electrode, *Ionics* 19 (2013) 1171–1177, <https://doi.org/10.1007/s11581-012-0839-0>.
- [31] G.A. Naikoo, T. Awan, H. Salim, F. Arshad, I.U. Hassan, M. Pedram, W. Ahmed, H. L. Faruck, A.A.A. Aljabali, V. Mishra, A. Serrano-Aroca, R. Goyal, P. Negi, M. Birkett, M.M. Nasef, N.B. Charbe, H.A. Bakshi, M.M. Tambuwala, Fourth-generation glucose sensors composed of copper nanostructures for diabetes management: a critical review, *Bioeng. Transl. Med.* 7 (2022) 10248, <https://doi.org/10.1002/btm2.10248>.
- [32] A.R. Amirsoleimani, H. Siampour, S. Abbasian, G.B. Rad, A. Moshaii, Z. Zaradshan, Copper oxide nanocolumns for high-sensitive non-enzymatic glucose sensing, *Sensing. Bio-Sensing Res.* 42 (2023) 100589, <https://doi.org/10.1016/j.sbsr.2023.100589>.
- [33] V. Jovanovski, N.I. Hrastnik, S.B. Hocevar, Copper film electrode for anodic stripping voltammetric determination of trace mercury and lead, *Electrochem. Commun.* 57 (2015) 1–4, <https://doi.org/10.1016/j.elecom.2015.04.018>.
- [34] L. Bie, X. Luo, L. Kang, D. He, P. Jiang, Commercial copper foam as an effective 3D porous electrode for nonenzymatic glucose detection, *Electroanalysis* 28 (2016) 2070–2074, <https://doi.org/10.1002/elan.201501167>.
- [35] A.O. Solak, P. Çekirdek, Square wave voltammetric determination of nitrate at a freshly copper plated glassy carbon electrode, *Anal. Lett.* 38 (2005) 271–280, <https://doi.org/10.1081/AL-200045149>.
- [36] A. Nyabadza, A. Plouze, S. Heidarinasab, M. Vazquez, D. Brabazon, Screen-printed electrodes on paper using copper nano- and micro-particles, *J. Mater. Res. Technol.* 29 (2024) 5189–5197, <https://doi.org/10.1016/j.jmrt.2024.03.016>.
- [37] P.S.L. Silva, D.A.G. Araujo, D.N. Medeiros, R.A. Ando, L.A. Pradela-Filho, T.R.L. C. Paixão, Copper electrodes via 3D printing and laser sintering fabrication for nonenzymatic glucose detection, *ACS Appl. Electron. Mater.* 7 (2025) 6520–6528, <https://doi.org/10.1021/acsaem.5c00862>.
- [38] J. Wasag, M. Grabarczyk, Copper film modified glassy carbon electrode and copper film with carbon nanotubes modified screen-printed electrode for the cd(II) determination, *Materials* 14 (2021) 5148, <https://doi.org/10.3390/ma14185148>.
- [39] H. Siddiqui, N. Singh, V. Chauhan, N. Sathish, S. Kumar, Electrochemical 3D printed copper garden for nitrate detection, *Mater. Lett.* 305 (2021) 130795, <https://doi.org/10.1016/j.matlet.2021.130795>.
- [40] H. Shamkhalichenar, C.J. Bueche, J.-W. Choi, Printed circuit board (PCB) technology for electrochemical sensors and sensing platforms, *Biosensors* 10 (2020) 159, <https://doi.org/10.3390/bios10110159>.
- [41] T.R.L.C. Paixao, J.L. Cardoso, M. Bertotti, Determination of nitrate in mineral water and sausage samples by using a renewable in situ copper modified electrode, *Talanta* 71 (2007) 186–191, <https://doi.org/10.1016/j.talanta.2006.03.040>.
- [42] C.R. Silva, C.D.C. Conceição, V.G. Bonifácio, O. Fatibello Filho, M.F.S. Teixeira, Determination of the chemical oxygen demand (COD) using a copper electrode: a clean alternative method, *J. Solid State Electrochem.* 13 (2009) 665–669, <https://doi.org/10.1007/s10008-008-0580-9>.
- [43] C. Guati, L. Gomez-Coma, M. Fallanza, I. Ortiz, Non-enzymatic amperometric glucose screen-printed sensors based on copper and copper oxide particles, *Appl. Sci.* 11 (2021) 10830, <https://doi.org/10.3390/app112210830>.
- [44] J.C.M. Gambo, R.C. Pena, T.R.L.C. Paixão, M. Bertotti, A renewable copper electrode as an amperometric flow detector for nitrate determination in mineral water and soft drink samples, *Talanta* 80 (2009) 581–585, <https://doi.org/10.1016/j.talanta.2009.07.028>.
- [45] S.-E. Bae, A.A. Gewirth, Differential reactivity of cu(111) and cu(100) during nitrate reduction in acid electrolyte, *Faraday Discuss.* 140 (2009) 113–123, <https://doi.org/10.1039/B803088J>.
- [46] B. Mukherjee, M. Mandal, R.R. Suresh, S. Kar, B.K. Parida, S. Chakraborty, G. Dutta, A non-enzymatic highly stable electrochemical sensing platform based on allylamine capped copper nanoparticles for the detection of the soil nitrate content, *Analyst* 150 (2025) 936–952, <https://doi.org/10.1039/d4an01345j>.
- [47] P. Mukherjee, M. Mandal, B. Mukherjee, G. Dutta, Nonenzymatic electrochemical sensor device for on-site nitrate determination using copper anchored magnetite nanocomposites, *Langmuir* 41 (2025) 6747–6758, <https://doi.org/10.1021/acs.langmuir.4c04903>.